Growth at High pH and Sodium and Potassium Tolerance in Media above the Cytoplasmic pH Depend on ENA ATPases in *Ustilago maydis*[▽]

Begoña Benito,[1] Blanca Garciadeblás,[1] José Pérez-Martín,[2] and Alonso Rodríguez-Navarro[1]*

Departamento de Biotecnología, Universidad Politécnica de Madrid, 28040 Madrid, Spain,[1] and Department of Microbial Biotechnology, Centro Nacional de Biotecnologia, CSIC, Campus de Cantoblanco, E-28049 Madrid, Spain[2]

Potassium and Na^+ effluxes across the plasma membrane are crucial processes for the ionic homeostasis of cells. In fungal cells, these effluxes are mediated by cation/H^+ antiporters and ENA ATPases. We have cloned and studied the functions of the two ENA ATPases of *Ustilago maydis*, *U. maydis* Ena1 (UmEna1) and UmEna2. UmEna1 is a typical K^+ or Na^+ efflux ATPase whose function is indispensable for growth at pH 9.0 and for even modest Na^+ or K^+ tolerances above pH 8.0. UmEna1 locates to the plasma membrane and has the characteristics of the low-Na^+/K^+-discrimination ENA ATPases. However, it still protects *U. maydis* cells in high-Na^+ media because Na^+ showed a low cytoplasmic toxicity. The UmEna2 ATPase is phylogenetically distant from UmEna1 and is located mainly at the endoplasmic reticulum. The function of UmEna2 is not clear, but we found that it shares several similarities with *Neurospora crassa* ENA2, which suggests that endomembrane ENA ATPases may exist in many fungi. The expression of *ena1* and *ena2* transcripts in *U. maydis* was enhanced at high pH and at high K^+ and Na^+ concentrations. We discuss that there are two modes of Na^+ tolerance in fungi: the high-Na^+-content mode, involving ENA ATPases with low Na^+/K^+ discrimination, as described here for *U. maydis*, and the low-Na^+-content mode, involving Na^+-specific ENA ATPases, as in *Neurospora crassa*.

Potassium is the most abundant cation in all types of living cells. Na^+, which is fairly abundant in many natural environments, can partially substitute for K^+ but becomes toxic above a certain Na^+/K^+ ratio (47). Therefore, the homeostatic processes that regulate the steady-state concentrations of K^+ and Na^+ in cells as well as the systems that mediate the transport of these cations across the plasma membrane and some endomembranes are crucial for maintaining cell viability. Among all the transport processes involved, K^+ and Na^+ effluxes play an indispensable role, and therefore, they take place in all types of living cells. For instance, in animal cells, an essential Na,K-ATPase that mediates Na^+ efflux and K^+ uptake consumes 20 to 30% of the produced ATP (33). Fungal and plant cells do not have this animal-type Na,K-ATPase (10), but K^+ or Na^+ efflux ATPases, also called ENA ATPases, are present in every fungal species (12) and have also been described for some bryophytes (15). ENA ATPases are phylogenetically close to but functionally different from animal Na,K-ATPases. Unlike the latter, ENA ATPases pump out almost every alkali cation and not exclusively Na^+, and they do not mediate K^+ uptake (14). The cation promiscuity of ENA ATPases may be an advantage in fungi because their membrane potential is very negative, and they can live in environments with high K^+ concentrations, such as plant tissues or plant debris. In these environments, the energetic conditions that prevail for K^+

efflux are similar to those prevailing for Na^+ efflux in Na^+ environments (12).

Fungal ENA ATPases are, in most cases, not essential in acidic environments because when the external pH is lower than the cytoplasmic pH, their function can be replaced by electroneutral Na^+/H^+ and K^+/H^+ antiporters. In these antiporters, which are universally present in eukaryotic cells, K^+ and Na^+ effluxes can be driven by the ΔpH (19). Consistent with these facts, the substitution of the *Saccharomyces cerevisiae* ENA1 (ScENA1) ATPase for the SOD2 antiporter of *Schizosaccharomyces pombe* (SpSOD2) (5) and the opposite substitution of the SpSOD2 antiporter for the ENA1 ATPase of *S. cerevisiae* (28) do not reveal any important functional advantage of the ATPase because these yeasts are acidophilic. Furthermore, the expression of SpSOD2 in plant cells (23, 57) apparently provides more benefits than the expression of ScENA1 (41). ENA ATPases are indispensable for growth when the Na^+ and K^+ concentrations are high in alkaline environments (8, 12), because in these environments, the transmembrane ΔpH would drive cation uptake instead of cation efflux if electroneutral antiporters are functional. Electrogenic antiporters can mediate membrane-potential-driven cation effluxes when the external pH is high, and in fact, they play a central role in bacteria growing at alkaline pH (43, 45). However, fungal electrogenic K^+ or Na^+/H^+ antiporters have not been described.

It is paradoxical that although ENA ATPases are indispensable only at a high pH, the most extensive studies of these ATPases have been performed with *S. cerevisiae* (49). This yeast is an acidophilic organism that is unable to grow at a high pH, in which the ENA ATPase is not essential for the above-mentioned reasons. Disruptions of *ENA* genes have also been

* Corresponding author. Mailing address: Departamento de Biotecnología, Universidad Politécnica de Madrid, 28040 Madrid, Spain. Phone: (34) 913365751. Fax: (34) 913365757. E-mail: alonso.rodriguez@upm.es.
[▽] Published ahead of print on 10 April 2009.

TABLE 1. Oligonucleotides used in this study[a]

Primer	5′–3′ sequence
ENA1-ATG	TCAGTTCAAGACAGCAGGTTCATC
ENA1-STOP	GCTACAGTGTGCTATGAAAGAAAG
XbaI-ENA2-ATG	GTCTAGATAAACAATGGTTCACGGTCATGGCT
ENA2-STOP	TGGCAGGACGGGGGAGACGCAATAC
NdeI-ENA1ATG	CCATATGGTGCACAAGAAAGAAGACAAG
NdeI-ENA1Rev	CCATATGTTTCACCATCGTTTTCTCGGTCGAGG
BamHI-ENA2ATG	GGGATCCTAAACAATGGTTCACGGTCATGGCT
NdeI-ENA2Rev	CCATATGTCTAGCAGTGGCGGCCGACTTTTC
PC-13B8-1	GGACACCTGGGGGAAGAACAAG
PC-13B8-1R	GGCCGGTGCAGACGAAGATGAT
PC-14G4-2	CTTTCATTGCCGTGGTCGAGCTGT
PC-14G4-2R	TTTTCGCTCAGTTGCTTCTTCGCC
UmACT1-2	GTGCCCATCTACGAAGGTTACT
UmACT1-1R	CGGCAGTGGTGGTGAAGGGGTAG
XbaNcENA2-ATG	GTCTAGAAAACAATGGGGGACAGAGATCGAACTT
NcENA2-STOP	TTCTTACACACCCTCTCCACCAACC
Bam-NcENA2Rev	CGGATCCTGTACACACCCTCTCCACCAACC

[a] In some of the primers, a restriction site sequence was included (underlined).

attained in *S. pombe* and *Schwanniomyces occidentalis*, but these disruptions do not resolve the uncertainties originated by the *S. cerevisiae* model. *S. pombe* is also acidophilic, and moreover, it has an atypical ENA ATPase, Cta3 (42), which mediates K^+ efflux almost exclusively (12). In the case of *S. occidentalis*, the double disruption of the two identified *ENA* genes was not attained (7). Moreover, its genome has not been sequenced, and the number of *ENA* genes is unknown.

In addition to the pending questions about the reasons for the universal presence of ENA ATPases in fungi (12) and their role in the growth of fungi at alkaline pH, new questions have been raised by the discovery of ENA ATPases in the parasites *Leishmania* and *Trypanosoma* (12, 31) and in bryophytes (15). Therefore, further studies of ENA ATPases are necessary, but the ENA ATPases of *S. cerevisiae* cannot serve as models, nor can the expression of foreign ENA ATPases be conveniently studied using *S. cerevisiae ena* mutants.

In the search for a new fungal model for studying ENA ATPases, we selected *Ustilago maydis*. *U. maydis* is a dimorphic basidiomycete plant pathogen (36) for which some studies of alkali cation transport (13) and cellular pH responses (3, 38) have already been carried out. In addition, it meets three important requirements: it grows at high pH values, its genome sequence is available (36), and it is amenable to easy molecular manipulations (35). Here we report the cloning and a functional study of the two ENA ATPases of *U. maydis*, *U. maydis* Ena1 (UmEna1) and UmEna2.

MATERIALS AND METHODS

Bacterial and fungal strains and growth conditions. *U. maydis* strains FB1 (*a1b1*) and FB2 (*a2b2*) (9) were used throughout this study. *Escherichia coli* strain DH5α was routinely used for the propagation of plasmids. The *S. cerevisiae* strains used were W303.1A (*Mat**a** ade2 ura3 trp1 leu2 his3*) and its derivatives B31 (*Mat**a** ade2 ura3 trp1 ena1-4Δ::HIS3 nha1Δ::LEU2*) (6) and G19 (*Mat**a** ade2 ura3 trp1 ena1-4Δ::HIS3*) (44), in which the Na^+ efflux systems ENA1-4 and NHA1 or only ENA1-4 is absent. Fungal strains were normally grown either in complex yeast-peptone-dextrose (YPD) medium (1% yeast extract, 2% peptone, 2% glucose) or in minimal SD medium (51). Growth at variable K^+ and Na^+ concentrations was done using arginine phosphate (AP) medium (48) supplemented with the indicated K^+ and Na^+ concentrations.

Recombinant DNA techniques. Manipulation of nucleic acids was performed by standard protocols or, when appropriate, according to the manufacturers'

instructions. PCRs were performed with a Perkin-Elmer thermocycler using the Expand-high-fidelity PCR system (Roche Molecular Biochemicals). Some of the PCR fragments were first cloned into the PCR2.1-TOPO vector using the TOPO TA cloning kit (Invitrogen). For expression in yeast cells, the genes were cloned into vector pYPGE15 (20). In all cases, most of the polylinker sequences preceding the translation initiation codon were eliminated, and a sequence environment as similar as possible to (A/U)A(A/C)A(A/C)AAUGUC(U/C) was created around it (29). DNA sequencing was performed using an automated ABI Prism 3730 DNA analyzer (Applied Biosystems). DNA and total RNA were prepared using the DNeasy and RNeasy plant kits (Qiagen), respectively. PCR amplifications of mRNA fragments were carried out on double-stranded cDNA synthesized from total RNA by using the cDNA synthesis system kit (GE Healthcare). The full-length *ena1* and *ena2* cDNAs were obtained by reverse transcription-PCR from RNA extracted from *U. maydis* using specific primers that amplified DNA fragments that contained the predicted start and stop codons (Table 1). The *ena1* and *ena2* genes were amplified from genomic DNA by PCR using the same primers that we used for the cDNAs.

Real-time PCR assays. The results reported in Table 2 were obtained using cells that were grown in AP medium with 3 mM KCl and then transferred into the same medium modified as follows: plus 10 mM tartaric acid and brought to pH 3.5 with arginine; with Ca^{2+} decreased to 0.5 mM and brought to pH 8.0 with arginine; plus 500 mM NaCl; plus 500 mM KCl; and without K^+. All treatments were for 2 h, except K^+ starvation, which was for 4 h. Real-time PCR assays were performed as described previously (26) except that the standard DNA solutions corresponded to the genes studied in this report, *ena1*, *ena2*, and actin genes of *U. maydis*. mRNA preparations were treated with RNase-free DNase I (40 U in 100 μl; Roche) for 1 h at 37°C. After treatment, mRNA was purified according to the instructions provided by the RNeasy plant kit (Qiagen). PCR primers UmACT1-2 (5′-GTGCCCATCTACGAAGGTTACT-3′) and UmACT1-1R (5′-CGGCAGTGGTGGTGAAGGGGTAG-3′) were designed to amplify the following fragments: *ena1* at positions 2952 to 3106 (GenBank accession number FM199940) and *ena2* at positions 3233 to 3359 (accession number FM199941).

TABLE 2. Effect of growth conditions on *U. maydis ena1* and *ena2* transcript abundances[a]

Transcript	Transcript abundance					
	YPD medium	AP plus 0.5 M Na$^+$	AP plus 0.5 M K$^+$	AP at pH 3.5	AP at pH 8.0	K$^+$ starvation
ena1	8.3	337	324	5.6	181	12.2
ena2	1.1	85	124	0.7	153	4.3

[a] Cells were grown overnight in AP medium with 3 mM K^+ and then transferred into the indicated media for 2 h. The given values are ratios with reference to actin transcript abundance.

Localization of UmEna1-green fluorescent protein (GFP) and UmEna2-GFP in *U. maydis* and *Neurospora crassa* ENA2 (NcENA2)-GFP in *Saccharomyces* yeast cells. The *ena1-GFP* and *ena2-GFP* constructs were in-frame fusions of the 3′ ends of the *ena1* and *ena2* open reading frames to the *GFP* gene of plasmid pCU3. To generate these constructs, full-length *ena1* cDNA was amplified using primers NdeI-ENA1ATG and NdeI-ENA1Rev, which include the NdeI restriction site. Full-length *ena2* cDNA was amplified using primers BamHI-ENA2ATG and NdeI-ENA2Rev, which include BamHI and NdeI restriction sites, respectively (Table 1).

For expression in *U. maydis*, *ena1* or *ena2* PCR fragments were cloned into the NdeI and NdeI/BamHI sites of plasmid pCU3 (P*tef1*-dependent expression), respectively, which are at the 5′ ends of the *GFP* gene. These plasmids were linearized with SspI and transformed into *U. maydis* cells to integrate the construct into the *cbx1* locus by homologous recombination as described previously (18). For expression in *S. cerevisiae*, the Nc*ena2-GFP* fusion was cloned into plasmid pYPGE15 (20). This construct was transformed into the above-mentioned B31 yeast mutant. To visualize the endoplasmic reticulum (ER), an ER-red fluorescent protein (RFP) fusion protein was produced as described previously (56) but using monomeric RFP as a reporter and a hygromycin resistance cassette as a selectable marker.

The GFP fluorescence signal in *U. maydis* and yeast cells was visualized using a confocal ultraspectral Leica (Mannheim, Germany) TCS-Sp2-AOBS-UV microscope.

Disruption of the *ena1* and *ena2* genes. To obtain the Δ*ena1* mutant, we constructed a disruption plasmid by ligating two DNA fragments of the *ena1* cDNA to the 5′ and 3′ ends of the nourseothricin resistance cassette in pNEBNat(+), a *U. maydis* integration vector (40). A 5′ fragment of 1,157 bp was obtained by digesting *ena1* cDNA with SpeI and BamHI and was inserted between the SpeI and BglII sites of plasmid pNEBNat(+). A 3′ fragment of 1,239 bp was obtained by digesting *ena1* cDNA with PvuII and HindIII and was inserted between the EcoRV and HindIII sites in plasmid pNEBNat(+). The plasmid with the two insertions was linearized with SspI and transformed into *U. maydis* wild-type strains FB1 and FB2. Transformants were selected in the presence of nourseothricin (Hans Knöll Institute, Jena, Germany) at 150 μg ml^{-1}.

The disruption plasmid for the Δ*ena2* mutant was constructed using fragments of the *ena2* gene for flanking the hygromycin B resistance cassette in plasmid pNEBHyg(+) (17). A 600-bp 5′ fragment was obtained by digesting *ena2* cDNA with SphI and BamHI and was inserted between the SphI and BamHI sites of pNEBHyg(+). A 920-bp 3′ fragment was obtained by digesting *ena2* cDNA with KpnI and EcoRI and was inserted between the KpnI and EcoRI sites of pNEBHyg(+). The plasmid with the two insertions was linearized with SphI and NarI and transformed into *U. maydis* wild-type strains FB1 and FB2. Transformants were selected in YPD medium supplemented with hygromycin B (Sigma-Aldrich) at 50 μg ml^{-1}.

The Δ*ena1* Δ*ena2* double mutant was constructed by transforming the Δ*ena1* strain with the linearized DNA construct used for the disruption of the Δ*ena2* strain. To recover the hygromycin B-resistant transformants, it was necessary to use regeneration agar (1 M sorbitol, 1% yeast extract, 2% peptone, 2% sucrose, and 1.5% agar) at pH 5.0 buffered with 20 mM MES (morpholineethanesulfonic acid). At other pH values, the Δ*ena1* Δ*ena2* mutant was never recovered.

The integration of plasmids into the corresponding loci was verified by PCR and Southern blot analyses in all cases. Southern blot analyses of the mutants were carried out according to standard procedures. Genomic DNA from the *U. maydis* mutants was digested with BstXI, SalI, EcoRI, or NcoI and hybridized with a probe that used either the antibiotic resistance cassette or fragments of the *ena1* or *ena2* gene, which did not show hybridization bands in the corresponding disrupted strains. The digoxigenin-labeled DNA probe was amplified by PCR. Hybridization and detection were carried out according to the supplier's instructions (Roche Applied Science).

Mating and virulence assays. To test for mating, strains were cospotted onto charcoal-containing potato dextrose plates that were sealed with Parafilm and incubated at 21°C for 48 h (30). For virulence assays, the maize cultivar Early Golden Bantam (Old Seeds, Madison, WI) was infected as described previously (27). The infection was repeated twice.

Na$^+$ and K$^+$ contents and intracellular distribution. *U. maydis* cells were collected by centrifugation, washed twice with K$^+$- and Na$^+$-free AP medium, and subsequently suspended in the same medium for 3 h. Cell samples were centrifuged, and total internal ions were extracted with 0.1 M HCl and analyzed by atomic emission spectrophotometry. The vacuolar Na$^+$/K$^+$ ratio was determined by treating the cells with digitonin, which selectively permeabilizes the plasma membrane (22, 34). Samples of cell suspensions incubated for 3 h in K$^+$- and Na$^+$-free AP medium were treated with 0.001% digitonin and 1 M sorbitol

in the same medium. At intervals, the cells were centrifuged at 8,000 × *g* for 1 min, and the supernatants containing the ions released by the digitonin treatment were analyzed by atomic emission spectrophotometry. The pellets were extracted with 0.1 M HCl to determine the K$^+$ and Na$^+$ contents that had not been released by the digitonin treatment. To ensure that during the digitonin treatment, the vacuolar membranes remained intact and able to maintain ΔpH, the accumulation of acridine orange [3,6-bis(dimethylamino)acridine] in the vacuole was monitored (22). This fluorescent dye penetrates the plasma membrane in an uncharged, neutral form and then accumulates into acidic organelles, where it is trapped in the protonated form. Previous to the digitonin treatment, the cells were incubated in AP medium with 100 μg ml^{-1} acridine orange for 20 min at room temperature. Next, 0.001% digitonin was added, and at intervals, 4 μl of the cell suspension was transferred onto a slide, covered with a cover glass, and observed with a Zeiss fluorescence microscope under blue light. Images were recorded with a Leica DFC300FX color camera connected to the microscope.

Na$^+$ efflux in *U. maydis* and yeast cells. *U. maydis* cells were grown overnight in AP medium supplemented with 30 mM K$^+$ and then Na$^+$ loaded by suspending the cells for 1 h in AP medium (pH 8.0) buffered with 10 mM TAPS (*N*-[Tris(hydroxymethyl)methyl]-3-aminopropanesulfonic acid) and containing either 200 or 50 mM NaCl for wild-type FB1 and Δ*ena1* Δ*ena2* mutant cells, respectively. The cells thus loaded with Na$^+$ were spun down and suspended in AP medium (pH 8.0) in the presence of 50 mM K$^+$ and 10 mM Na$^+$. At intervals, samples of the suspended cells were filtered, washed, and extracted with 0.1 M HCl. For *S. cerevisiae*, B31 yeast transformants were grown overnight in AP medium supplemented with 3 mM K$^+$. Cells were then Na$^+$ loaded into a solution containing 10 mM TAPS (pH 8.0), 100 mM NaCl, 1 mM MgCl$_2$, and 2% glucose for 1 h. The Na$^+$-loaded cells were spun down and suspended in a solution containing TAPS (pH 8.0), 50 mM K$^+$, and 2% glucose. At intervals, samples of the suspended cells were filtered and washed, and HCl was extracted. In both *U. maydis* and yeast cells, cation contents were determined from atomic emission spectrophotometric analyses of the extracts. For each experiment, three independent repetitions were carried out.

Protein alignments and generation of phylogenetic trees. Protein sequence alignments and phylogenetic trees were obtained using the Clustal X program (54).

Nucleotide sequence accession numbers. Sequence data have been deposited in the GenBank database under accession numbers FM199940 for *ena1* and FM199941 for *ena2*.

RESULTS

Basic description of *U. maydis* alkali cation tolerance. *U. maydis* grew well in a wide range of Na$^+$ or K$^+$ concentrations at pH values ranging from 3.5 to 9.0. In YPD medium, it grew in up to 1.0 M Na$^+$ or 1.2 M K$^+$. Growth was also maintained at low-micromolar K$^+$ and Na$^+$ concentrations, where both cations were depleted down to almost undetectable concentrations (13). In mineral AP medium, the toxic effect of Na$^+$ was almost independent from the K$^+$ concentration; for example, growth rates at 150 mM Na$^+$ with either 4.5 or 0.5 mM K$^+$ were almost identical. At 4.5 mM K$^+$, the growth rate was not affected by 500 mM Na$^+$ and was only partially reduced by 800 mM Na$^+$.

Analyses of cation contents of *U. maydis* cells growing at high Na$^+$ concentrations revealed that they contained fairly high internal Na$^+$/K$^+$ molar ratios without any apparent detrimental effect. These results raised the question of whether Na$^+$ was sequestered into the vacuole as in plant cells (21, 53). To address this question, we determined the cytoplasmic Na$^+$/K$^+$ ratio by measuring the Na$^+$ and K$^+$ losses after digitonin permeabilization of the plasma membrane. The accuracy of the results of this approach relies on two conditions, that tonoplasts were not permeabilized and that intact cells did not take up the K$^+$ released by permeabilized cells. To test the integrity of the tonoplast, we checked the capacity of the vacuoles to maintain ΔpH by acridine orange staining (2, 22). A significant effect of digitonin on the tonoplast was found to
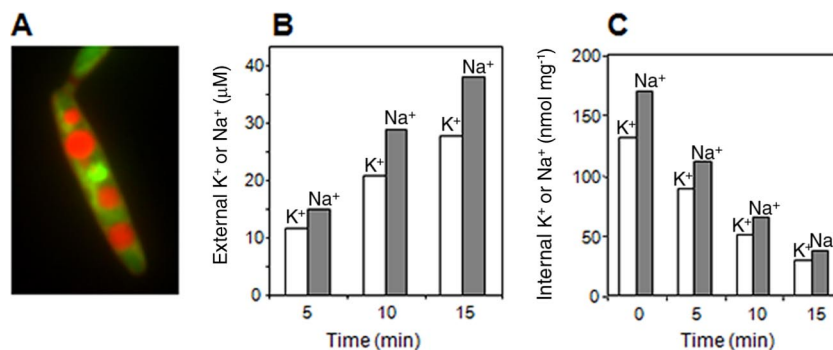
FIG. 1. Molar Na$^+$/K$^+$ ratios in the cytoplasm of *U. maydis*. (A) Acridine orange staining of *U. maydis* vacuoles after 15 min of treatment with digitonin. (B) Time course of Na$^+$ and K$^+$ release after digitonin permeabilization of the plasma membrane. (C) Time course of Na$^+$ and K$^+$ contents of cells under conditions of digitonin treatment.

start after 20 min of treatment. Therefore, in the experiments that we report below, the time of digitonin treatment was limited to 15 min so that not more than 1 vacuole out of 100 was unstained. To check that the K$^+$ released by permeabilized cells was not taken up by intact cells during the experiments, we carried out parallel experiments in the presence and in the absence of antimycin A, which inhibits respiration and, consequently, K$^+$ uptake (46). The presence of this inhibitor did not affect the results. Furthermore, the time courses of the K$^+$ and Na$^+$ releases showed a constant Na$^+$/K$^+$ ratio from the first sample taken, with less than 10% of the cells permeabilized, up to the last sample taken, with probably more than 80% of the cells permeabilized. This result also ruled out the possibility that intact cells took up K$^+$.

U. maydis vacuoles were not stained by acridine orange in cells growing at high Na$^+$ concentrations (for example, 4.5 mM K$^+$/150 mM Na$^+$). This might be the result of an excessive uptake of cations and alkalinization of the cells, but the causes were not investigated. Incubation of these cells in K$^+$- and Na$^+$-free medium for 3 h did not change their K$^+$ and Na$^+$ contents significantly but fully restored the capacity of the vacuoles to accumulate acridine orange (Fig. 1A). An additional advantage of this incubation was that *U. maydis* cells adapted to keeping very low K$^+$ or Na$^+$ concentrations in the external medium (typically, 0.5 µM K$^+$ and 10 µM Na$^+$). Under these conditions, it was very simple to measure the K$^+$ and Na$^+$ released into the external medium by the digitonin treatment because the treatment increased the external concentrations very much, while untreated cells kept them very low.

Our results with cells grown at different K$^+$ and Na$^+$ concentrations show that the vacuole of *U. maydis* did not accumulate large amounts of Na$^+$. When cells grown at 4.5 mM K$^+$ and 150 mM Na$^+$ and subsequently K$^+$ and Na$^+$ starved for 3 h were treated with digitonin, the time courses of the K$^+$ and Na$^+$ releases into the external medium showed a permanent increase at a constant Na$^+$/K$^+$ ratio of 1.4 (Fig. 1B). At the same time, the ratio between the Na$^+$ and K$^+$ that remained in the cells (vacuolar content of permeabilized cells plus the content of intact cells) after each interval treatment decreased permanently (Fig. 1C). In three independent experiments with cells grown at 4.5 mM K$^+$ and 150 mM Na$^+$, the mean Na$^+$/K$^+$ ratio was 1.5 ± 0.2, while in cells grown at 10 mM K$^+$ and 500 mM Na$^+$, the mean ratio was 2.3 ± 0.2. Taken together, these

experiments indicated that the Na$^+$/K$^+$ ratio in the vacuole of actively growing cells was lower than the cytoplasmic Na$^+$/K$^+$ ratio and that the latter could be as high as 2.3 without any detrimental effect.

***U. maydis* has two ENA ATPases.** Computer-based searches of the genomic sequence of *U. maydis* using ENA ATPase sequences as queries identified two open reading frames that could encode Ena proteins. The corresponding genes, *ena1* and *ena2*, were cloned by a standard PCR-based approach. These genes did not contain introns and encode two proteins of 1,100 and 1,125 amino acids, respectively. The study of the amino acid sequences of both ATPases showed that their structures and functional characteristics corresponded to typical P-type ATPases (33, 50) of group IID (4). Remarkably, the *ena1* and *ena2* genes did not result from a recent duplication event because the phylogenetic distance between the encoded pumps was larger than the phylogenetic distance between the basidiomycete UmEna1 and the ascomycete NcENA1 pumps. The existence of two or more ENA ATPases in two distant phylogenetic clusters was also found for *Aspergillus*, *Neurospora*, and *Magnaporthe* (Fig. 2). The *ena1* gene was located on chromosome 3, and the *ena2* gene was located on chromosome 1. Transcript expressions of *ena1* and *ena2* as determined by real-time PCR showed that the levels of expression of both genes were low under normal conditions and that almost a 100-fold induction occurred at high Na$^+$ or K$^+$ concentrations or at a high pH (Table 2), which is very similar to previous descriptions of other fungi (1, 7, 11, 25).

The *ena1* and *ena2* genes were then expressed in mutant yeast strain B31, which lacks the ENA ATPases and the NHA1 antiporter (8), using yeast expression vector pYPGE15 with the genes under the control of the *PGK1* gene promoter (20). *ena1* but not *ena2* completely suppressed the defective growth of B31 at high Na$^+$ and high K$^+$ concentrations (Fig. 3A). However, *ena2* suppressed the defect of B31 only at the minimal Na$^+$ concentration at which the growth of B31 was inhibited. Consistent with the pumping capacities of an Na-ATPase, UmEna1 mediated the cellular Na$^+$ loss at pH 8.0 with 10 mM Na$^+$ in the external medium (Fig. 3B). Under these conditions, an Na$^+$ channel or an electroneutral Na$^+$/H$^+$ antiporter would mediate Na$^+$ uptake driven by the membrane potential and ΔpH, respectively. ENA ATPases may be specific for K$^+$ or Na$^+$, protecting cells only from high concentrations of one of
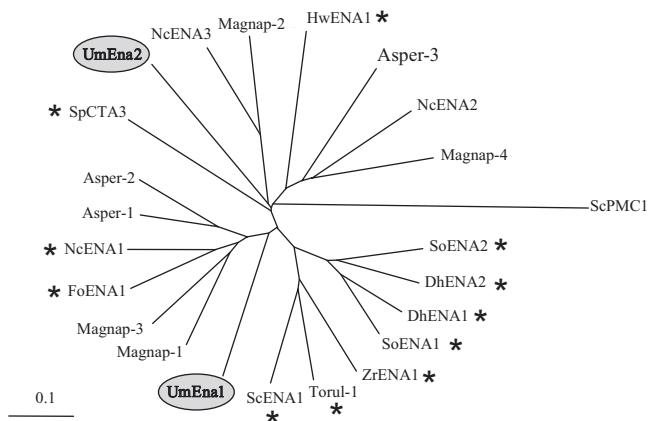
FIG. 2. Phylogenetic tree of fungal ENA ATPases. Species are as follows: ScPMC1, *Saccharomyces cerevisiae* Ca^{2+}-ATPase included as an outgroup (GenBank accession number P38929); UmEna2, *Ustilago maydis* (accession number XP_756351); HwENA1, *Hortaea werneckii* (accession number ABD64570); NcENA2, *Neurospora crassa* (accession number AJ243519); Magnap-4, *Magnaporthe grisea* (accession number XP_001404752); Asperg-3, *Aspergillus fumigatus* (accession number EAL87230); SoENA1, *Schwanniomyces occidentalis* (accession number AAB86426); DhENA1, *Debaryomyces hansenii* (accession number AAK28385); DhENA2, *D. hansenii* (accession number AAK52600); SoENA2, *S. occidentalis* (accession number AAB86427); ZrENA1, *Zygosaccharomyces rouxii* (accession number BAA11411); ScENA1, *S. cerevisiae* (accession number P13587); Torul-1, *Torulaspora delbrueckii* (accession number AAZ04389); Magnap-3, *M. grisea* (accession number XP_365372); Magnap-1, *M. grisea* (accession number XP_360418); NcENA1, *N. crassa* (accession number AJ243520); FoENA1, *Fusarium oxysporum* (accession number AAR01872); Asperg-2, *A. fumigatus* (accession number EAL85670); Asperg-1, *A. fumigatus* (accession number EAL89843); UmEna1, *U. maydis* (accession number XP_757891); SpCTA3, *Schizosaccharomyces pombe* (accession number NP_595246); Magnap-2, *M. grisea* (accession number XP_359699); NcENA3, *N. crassa* (accession number XP_962099). An ∗ indicates cloned pumps.

these cations, or nonspecific, protecting cells from high concentrations of either of them (12). The results showed that UmEna1 belonged to the nonspecific group (Fig. 3A).

Effects of the disruption of *ena1* and *ena2*. The function of the UmEna1 and UmEna2 ATPases was assessed by gene disruption. Initially, we obtained the single and double disruptions in strain FB1, which is almost identical to the strain whose genome has been sequenced (36). Later, the disruptions were also attained in a strain of the opposite mating type, FB2, which is suited to performing plate mating assays and plant infection studies. The disruptions of the *ena1* and *ena2* genes in either FB1 or FB2 produced identical results, and only the results obtained with strain FB1 are presented. Disruptions were checked by Southern blot analyses, which proved that the *ena1* or *ena2* gene had been disrupted (data not shown).

Consistent with the established function of ENA ATPases (12) and the previously discussed functional expression of the UmEna1 and UmEna2 ATPases in yeast cells (Fig. 3), clear defects in growth and Na$^+$/K$^+$ tolerance of the *U. maydis* Δ*ena1* Δ*ena2* strain became evident at high pH values. At pH 5.0, the Δ*ena1* Δ*ena2* double mutant was as tolerant as the wild-type strain (similar levels of growth at 800 mM Na$^+$ or 1 M K$^+$ in YPD medium) (data not shown). In contrast, at pH
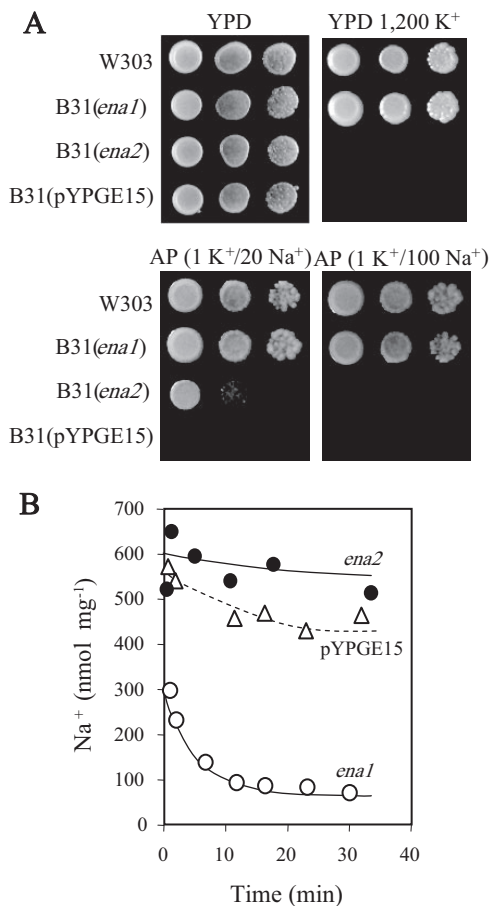

FIG. 3. Functional expression of *ena1* and *ena2* cDNAs in *S. cerevisiae*. (A) Suppression of the defective growth of Na$^+$ efflux mutant strain B31 in the presence of high Na$^+$ or K$^+$ concentrations; drops of serial dilutions of cell suspensions of the wild type and of the B31 strain transformed with the empty plasmid or with the *ena1* or *ena2* cDNAs were inoculated into the indicated media. Numbers indicate concentrations (mM). (B) Time courses of Na$^+$ extrusion at pH 8.0 in B31 transformants loaded with Na$^+$. B31 was transformed with the empty plasmid (open triangles), *ena1* (open circles), and *ena2* (closed circles).

8.0, the Δ*ena1* Δ*ena2* double mutant was inhibited by Na$^+$ concentrations as low as 20 mM in mineral AP medium (Fig. 4A). Remarkably, at pH 9.0, the Δ*ena1* Δ*ena2* mutant failed to grow either in YPD medium without the addition of Na$^+$ or K$^+$ (data not shown) or in 1 mM K$^+$ AP medium (Fig. 4A). Most of the defects in the Δ*ena1* Δ*ena2* double mutant were accounted for by the Δ*ena1* mutation. The effects of the Δ*ena2* mutation on Na$^+$ or K$^+$ tolerance were almost undetectable both in the wild type and in the Δ*ena1* strain (Fig. 4A). As expected from these results, the lack of the ENA ATPases abolished Na$^+$ efflux at high pH values (Fig. 4B).

UmEna1p and UmEna2p show a different endosomal/plasma membrane distribution. Some eukaryotic Na$^+$/H$^+$ exchangers show dual endosomal/plasma membrane distribution (19). Moreover, considering the phylogenetic divergence of the UmENA1 and UmEna2 ATPases (Fig. 2) and our failure to detect a clear function of UmEna2, the localization of UmEna2 could not be predicted. Therefore, we checked the cellular locations of the UmEna1-GFP and UmEna2-GFP pro-
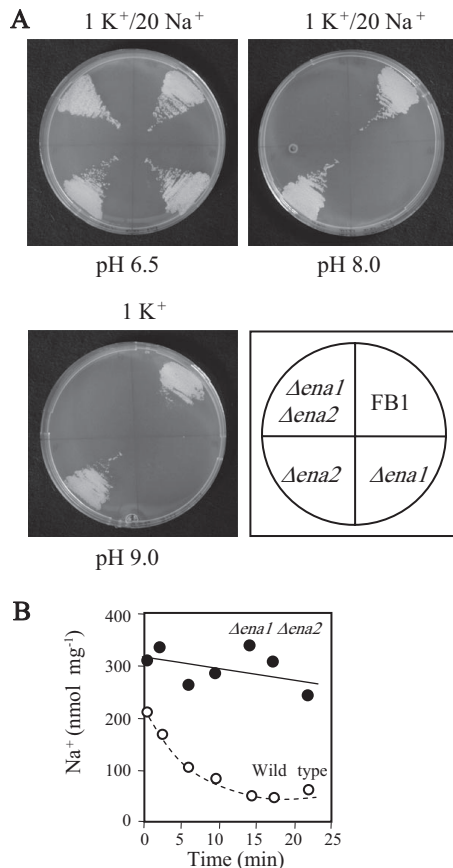
FIG. 4. Defects of Δena1 and Δena2 mutants. (A) Growth defects in AP medium at different pH values and different Na$^+$ concentrations, as indicated. Numbers indicate concentrations (mM). (B) Na$^+$ extrusion from Na$^+$-loaded cells in AP medium at pH 8.0 with 50 mM KCl and 10 mM NaCl.

FIG. 5. Localization of UmEna1-GFP and of UmEna2-GFP fusion proteins in U. maydis Δena1 and Δena2 mutants, respectively. (A to C) Images of the Δena1 strain expressing the UmEna1-GFP fusion protein. (A) GFP fluorescence; (B) differential interference contrast (DIC) image; (C) merge of the GFP signal and the DIC image. (D to G) Images of the Δena2 strain expressing the UmEna2-GFP and ER-RFP fusion proteins. (D) DIC image; (E) GFP fluorescence; (F) RFP fluorescence; (G) merge of the GFP and RFP signals.

teins in U. maydis cells with gene expression under the control of the transcriptional elongation factor promoter (18). The GFP fusions did not affect the above-described biological activities of the UmEna1 and UmEna2 ATPases. The expression of UmEna1-GFP in the Δena1 strain suppressed its sensitivity to high Na$^+$ or K$^+$ concentrations (Fig. 4A), and the expression of UmEna2-GFP in mutant yeast strain B31 weakly suppressed its Na$^+$ sensitivity (Fig. 3A).

Microscopy analysis of U. maydis cells expressing UmEna1-GFP located the protein mainly to the plasma membrane and to some vesicles, which might be in transit to the plasma membrane (Fig. 5). In contrast, UmEna2-GFP was located around the nucleus, in close proximity to the plasma membrane, and in internal vesicles. The coexpression of UmEna2-GFP with an ER-RFP fusion demonstrated that UmEna2-GFP localized to the ER and to other endomembranes that were not investigated (Fig. 5).

NcENA2 has similarities with UmEna2. In a previous report, the function of the NcENA2 ATPase (previously called ph7) could not be established (11). Interestingly, the phylogenetic divergence between the NcENA1 and NcENA2 ATPases was similar to that between the UmEna1 and UmEna2 ATPases (Fig. 2). Now, using a new construct in which the
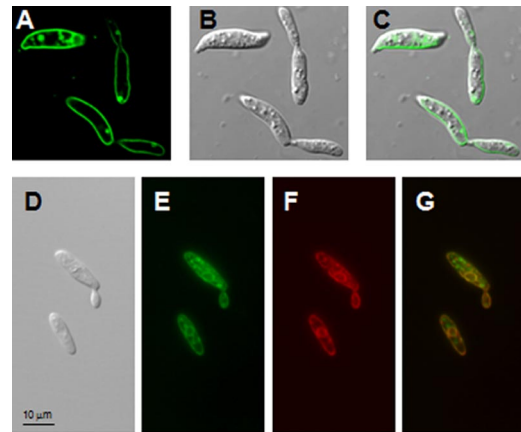
sequence context around the first in-frame AUG was optimized for translation, we found that NcENA2 weakly suppressed the defect of the B31 mutant, exactly as shown for UmEna2 in Fig. 3A (data not shown). Next, to investigate whether NcENA2 was located to the plasma membrane or to endomembranes, we expressed the NcENA2-GFP fusion protein in yeast cells. The NcENA2-GFP signal localized to spots that were neither in the tonoplast nor in the plasma membrane. Although NcENA2 resembled UmEna2 in that both proteins show similar levels of functional expression in yeast cells and localized to endomembranes, they might fulfill different functions because the microscopic images of NcENA2-GFP did not correspond to a typical ER location (Fig. 6). N. crassa has a third ENA ATPase (NcENA3) (Fig. 2) that might be a functional homolog of UmEna2. This possibility was not tested because we have so far failed to clone NcENA3.

Do ENA ATPases have functions other than cation pumping in the plasma membrane? ENA ATPases are universally present in fungi, and many fungi have ENA genes that encode phylogenetically distant ENA ATPases (for example, U. maydis, Aspergillus fumigatus, and N. crassa ENA ATPases) (Fig. 2), which apparently locate to different membranes (Fig. 5 and 6). All these observations raised the question of whether the functions of ENA ATPases may be more than the currently
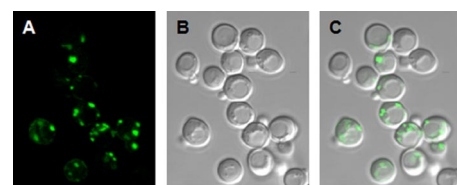

FIG. 6. Localization of the NcENA2-GFP fusion proteins in B31 yeast cells. Shown are images of the NcENA2-GFP fusion protein. (A) GFP fluorescence; (B) DIC image; (C) merge of the GFP signal and the DIC image.
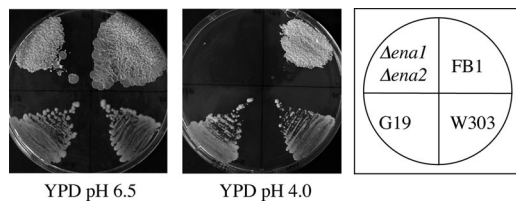
FIG. 7. Defective growth of the *U. maydis* Δ*ena1* Δ*ena2* strain in YPD medium at pH 4.0. The wild-type strain of *U. maydis* (FB1) and the wild-type and Δ*ena1-4* (G19) strains of *S. cerevisiae* were used as controls.

assigned roles of Na^+ and K^+ pumping out of cytoplasm. Therefore, we selected several physiological functions with no obvious relationship to ion transport to be tested in the Δ*ena1* and Δ*ena2* strains.

First, we tested the mating abilities of the single and double mutants of the FB1 and FB2 strains. All mixtures of sexually compatible strains developed positive Fuz reactions regardless of the Δ*ena1* or Δ*ena2* mutation (not shown). The virulence capability of the Δ*ena* strains was also tested by the inoculation of mixtures of sexually compatible mutants (FB1 Δ*ena1*/FB2 Δ*ena1*, FB1 Δ*ena2*/FB2 Δ*ena2*, and FB1 Δ*ena1* Δ*ena2*/FB2 Δ*ena1* Δ*ena2*) or wild-type strains (FB1/FB2) onto maize seedlings. Mixtures of mutants did not show any difference in virulence symptoms such as chlorosis, anthocyanin pigmentation, or tumor production compared to those of wild-type mixtures (not shown).

Next, we carried out growth tests under many different conditions and found a surprising defect. The growth of *U. maydis* was slightly inhibited in YPD medium (1% yeast extract, 2% peptone), as used in yeast research (51), at pH 4.0 or lower. In contrast, the Δ*ena1* Δ*ena2* double mutant strain was completely unable to grow in YPD medium at pH 4.0 (Fig. 7), while the Δ*ena1* and Δ*ena2* single mutant strains grew identically to the wild-type strain. Different types of commercial peptones added to AP medium reproduced the YPD effect, but vitamin-free Casamino Acids (Difco) produced only a weak effect. The marked pH dependence of the toxic effect suggested that the permeable form of a fatty acid might be involved, but we failed to find a fatty acid or a mixture of fatty acids that produced the inhibition. We also tested whether the addition of NH_4^+ suppressed the inhibitory effect, finding that concentrations of up to 200 mM did not show any suppressive effect (data not shown). The defective growth at pH 4.0 in YPD medium produced by the Δ*ena1* Δ*ena2* mutations in *U. maydis* was not produced by the equivalent Δ*ena1-4* mutation in *S. cerevisiae* (Fig. 7).

DISCUSSION

Low Na^+ toxicity in *U. maydis*. It is normally assumed that K^+ is the most abundant cellular cation and that cells growing in the presence of Na^+, as do animal cells, exclude Na^+ to keep a high K^+ content. Under similar conditions, plant cells also sequester Na^+ in the vacuole to keep a low Na^+/K^+ ratio in the cytoplasm (21, 53). The notion that the concentration of Na^+ is low in the cytoplasm does not apply to *U. maydis*. We

observed good growth when the cytoplasmic Na^+/K^+ ratio was 2.3.

The inability of fungal cells to decrease the cytoplasmic Na^+ concentration by accumulating it into the vacuole, as reported here for *U. maydis*, was previously reported for *S. cerevisiae* (39, 46, 55) and *Debaryomyces hansenii* (39). These three species grow normally with a rather high Na^+ content, exhibiting low cytoplasmic Na^+ toxicity. In *S. cerevisiae*, an Na^+/K^+ ratio of 1 is completely nontoxic (39), and in *D. hansenii*, the Na^+/K^+ ratio can be as high as 4 without detrimental effects (39). Similarly, *Hortaea werneckii* and *Aureobasidium pullulans* show comparable K^+ and Na^+ contents when actively growing at 0.8 M NaCl (37). In contrast, in *Neurospora crassa* (52), *Candida albicans* (16), and *Candida tropicalis* (24), low Na^+ contents are toxic, which suggests high cytoplasmic Na^+ toxicity.

In summary, there seem to be two types of fungi regarding Na^+ tolerance, those tolerant to high Na^+ contents in the cytoplasm, which include *U. maydis*, and those intolerant to high Na^+ contents.

Role of UmEna1 in the plasma membrane. The functional expression of the UmEna1 ATPase in an Na^+ efflux-defective strain of *S. cerevisiae* and the defects of the *U. maydis* Δ*ena1* and Δ*ena1* Δ*ena2* strains indicate that UmEna1 is a typical ENA ATPase (12). Its main function is to pump Na^+ and K^+ out of the cytoplasm, especially at high pH values, where the transcripts of these ATPases exhibit maximal levels (Table 2) (1, 7, 11, 25). At pH 8.0, UmEna1 was necessary even for modest Na^+ or K^+ tolerances, and more remarkable still, UmEna1 was required for growth at pH 9.0 even when Na^+ or K^+ concentrations were low (Fig. 4A). This specific requirement of ENA ATPases for the growth of fungi in high-pH media has been suspected for a long time (12) but had not been demonstrated previously.

The basic explanation for the variable requirements of ENA ATPases in alkaline-pH media depending on the Na^+ and K^+ concentrations in the external media is that the homeostasis of the K^+ and Na^+ levels in the cytoplasm depends on K^+ and Na^+ effluxes. Fungi possess K^+ or Na^+/H^+ antiporters (*U. maydis* has an *nha1* gene, which encodes a protein that is highly similar in sequence to the ScNHA1 antiporter) (our unpublished results) and ENA ATPases (12), but fungal electrogenic antiporters have not been reported. ATPases can function at any pH of the external medium, but this is not the case for electroneutral antiporters, which depend on an acidic external medium to function optimally. At external pH values above the cytoplasmic pH, they may mediate Na^+ or K^+ efflux but only if the concentration of the corresponding cation is lower in the external medium than in the cytoplasm.

UmEna1 is a pump of low Na^+/K^+ discrimination, like many of the fungal ENA ATPases studied so far (12). The effectivenesses of these ATPases in mediating Na^+ tolerance must necessarily be linked to a low cytoplasmic toxicity of Na^+, because an ENA ATPase of low Na^+/K^+ discrimination cannot keep a low molar Na^+/K^+ ratio in the cytoplasm. A low Na^+/K^+ ratio has to be maintained by *Neurospora crassa* because it stops growing when Na^+ and K^+ contents reach an Na^+/K^+ ratio that is much lower than 1 (52). In accordance with this requirement, *N. crassa* is furnished with an Na^+-specific ENA ATPase that does not protect cells from high K^+

concentrations (12). As mentioned above, *D. hansenii* (39), *U. maydis* (Fig. 1), and *S. cerevisiae* (39) are not affected by cytoplasmic molar Na^+/K^+ ratios of 4, 2, and 1, respectively. Therefore, because their ENA ATPases do not discriminate between Na^+ and K^+, they provide protection against high concentrations of any of these cations (Fig. 3A) (1, 12). The most plausible hypothesis that can be put forward at this moment is that high-Na^+-content fungi possess ENA ATPases of low Na^+/K^+ discrimination and that low-Na^+-content fungi possess Na^+-specific ENA ATPases. This further implies that the general idea that considers Na^+ to be highly toxic in the cytoplasm needs to be revised, at least for fungi.

Expression of UmEna2p and NcENA2p in endosomal membranes. The UmEna2 and UmEna1 ATPases are in different phylogenetic clusters of the ENA phylogenetic tree. The same occurs with the ENA ATPases of *N. crassa* and with those of *Aspergillus fumigatus* and *Magnaporthe grisea*, although in the latter two species, the ATPases have not been cloned and studied (Fig. 2). Because the phylogenetic distances between UmEna1 and UmEna2 and between NcENA1 and NcENA2 are greater than that between UmEna1 and NcENA1, it can be concluded that a common ancestor of ascomycetous and basidiomycetous fungi has already had at least two types of ENA ATPases. The conservation of ENA ATPases in two phylogenetic clusters in *U. maydis* and *A. fumigatus* and in three clusters in *N. crassa* and *M. grisea* (Fig. 2) suggests the existence of ENA ATPases with different cellular functions. A similar suggestion can be derived from the different membranes to which UmEna1 and UmEna2 locate (Fig. 5). The locations of NcENA1 and NcENA2 have not been established. However, in *S. cerevisiae*, NcENA1 mediates rapid Na^+ effluxes (11) that are exclusively compatible with a plasma membrane location, and the expression of NcENA2-GFP in yeast cells strongly suggests that it locates to endomembranes (Fig. 6) resembling UmEna2. NcENA2 and UmEna2 increased the Na^+ tolerance of the Na^+ efflux-defective *S. cerevisiae* mutant very slightly. Such a weak effect cannot be directly attributed to an increase in Na^+ efflux, which, if it actually occurred, would be very weak and untestable, but supports that they are Na^+ ATPases. Furthermore, the expression patterns of UmEna2 and NcENA2 (see Table 2 and reference 11, respectively) and the conservation of the typical motifs of ENA ATPases suggest that they pump Na^+ and K^+, as plasma membrane ENA ATPases do. In summary, taking all these observations together, it seems that UmEna2 and NcENA2 mediate Na^+ or K^+ fluxes in the ER or in other endomembranes.

The $\Delta ena2$ mutation did not produce any detectable defect except for the lack of growth in peptone at low pH values in the $\Delta ena1$ strain. Our failure to identify which compound in peptone was toxic makes it impossible to predict the defective function that produced the toxicity of peptones. However, as discussed above, the defective function may occur in internal membranes. Because this defective function occurred only in the $\Delta ena1 \Delta ena2$ double mutant, UmEna1 must also be involved in the function. To accomplish this, UmEna1 must cycle between endomembranes and the plasma membrane, as previously described for Na^+/H^+ exchangers (19). Consistent with this possibility, the overexpression of the moss *Physcomitrella patens* ENA1 ATPase in rice and barley produces changes in metabolite levels that are difficult to predict based solely on the

known function of this ATPase to pump Na^+ or K^+ out of the plasma membrane (15). Citric, isocitric, and aconitic acid levels were consistently reduced in both species (32), which indicates that peroxisome function is affected.

It appears that ENA ATPases fulfill more functions than just that of cation pumping across the plasma membrane. In *U. maydis* and *N. crassa*, different functions of ATPases in different phylogenetic clusters may be shared to different degrees. The same might occur in other fungi, such as *Aspergillus* or *Magnaporthe*, with ATPases in different phylogenetic clusters (Fig. 2). In the case of *Saccharomyces*, *Schwanniomyces*, *Zygosaccharomyces* (Fig. 2), and *Physcomitrella* (15), in which two or more ENA ATPases in the same species are in the same phylogenetic cluster, different functions might be carried out by the same ATPase or by ATPases that are phylogenetically close.

REFERENCES

1. **Almagro, A., C. Prista, B. Benito, M. C. Loureiro-Dias, and J. Ramos.** 2001. Cloning and expression of two genes coding for sodium pumps in the salt-tolerant yeast *Debaryomyces hansenii*. J. Bacteriol. **183:**3251–3255.
2. **Anderson, R., and L. Orci.** 1988. A view of acidic intracellular compartments. J. Cell Biol. **106:**539–543.
3. **Aréchiga-Carvajal, E. T., and J. Ruiz-Herrera.** 2005. The RIM101/*pacC* homologue from the basidiomycete *Ustilago maydis* is functional in multiple pH-sensitive phenomena. Eukaryot. Cell **4:**999–1008.
4. **Axelsen, K. B., and M. G. Palmgren.** 1998. Evolution of substrate specificities in the P-type ATPase superfamily. J. Mol. Evol. **46:**84–101.
5. **Bañuelos, M. A., F. J. Quintero, and A. Rodríguez-Navarro.** 1995. Functional expression of the ENA1 (PMR2)-ATPase of *Saccharomyces cerevisiae* in *Schizosaccharomyces pombe*. Biochim. Biophys. Acta **1229:**233–238.
6. **Bañuelos, M. A., J. Ramos, F. Calero, V. Braun, and S. Potier.** 2002. Cation/H^+ antiporters mediate potassium and sodium fluxes in *Pichia sorbitophila*. Cloning of the *PsHHA1* and *PsNHA2* genes and expression in *Saccharomyces cerevisiae*. Yeast **19:**1365–1372.
7. **Bañuelos, M. A., and A. Rodríguez-Navarro.** 1998. P-type ATPases mediate sodium and potassium effluxes in *Schwanniomyces occidentalis*. J. Biol. Chem. **273:**1640–1646.
8. **Bañuelos, M. A., H. Synchrová, C. Bleykasten-Grosshans, J.-L. Souciet, and S. Potier.** 1998. The Nha1 antiporter of *Saccharomyces cerevisiae* mediates sodium and potassium efflux. Microbiology **144:**2749–2758.
9. **Banuett, F., and I. Herskowitz.** 1989. Different *a* allels of *Ustilago maydis* are necessary for maintenance of filamentous growth but not for meiosis. Proc. Natl. Acad. Sci. USA **86:**5878–5882.
10. **Barrero-Gil, J., B. Garciadeblás, and B. Benito.** 2005. Sodium, potassium-ATPases in algae and oomycetes. J. Bioenerg. Biomembr. **37:**269–278.
11. **Benito, B., B. Garciadeblas, and A. Rodríguez-Navarro.** 2000. Molecular cloning of the calcium and sodium ATPases in *Neurospora crassa*. Mol. Microbiol. **35:**1079–1088.
12. **Benito, B., B. Garciadeblás, and A. Rodríguez-Navarro.** 2002. Potassium- or sodium-efflux ATPase, a key enzyme in the evolution of fungi. Microbiology **148:**933–941.
13. **Benito, B., B. Garciadeblás, P. Schreier, and A. Rodríguez-Navarro.** 2004. Novel P-type ATPases mediate high-affinity potassium or sodium uptake in fungi. Eukaryot. Cell **3:**359–368.
14. **Benito, B., F. J. Quintero, and A. Rodríguez-Navarro.** 1997. Overexpression of the sodium ATPase of *Saccharomyces cerevisiae*. Conditions for phosphorylation from ATP and P_i. Biochim. Biophys. Acta **1328:**214–225.
15. **Benito, B., and A. Rodríguez-Navarro.** 2003. Molecular cloning and characterization of a sodium-pump ATPase of the moss Physcomitrella patens. Plant J. **36:**382–389.
16. **Biswas, S. K., K. Yokoyama, K. Nishimura, and M. Miyaji.** 2000. Effect of pH, carbon source and K^+ on the Na^+-inhibited germ tube formation of *Candida albicans*. Med. Microbiol. **38:**363–369.
17. **Bölker, M., H. U. Böhnert, K. H. Brown, J. Görl, and R. Kahmann.** 1995. Tagging pathogenicity genes in *Ustilago maydis* by restriction enzyme-mediated integration (REMI). Mol. Gen. Genet. **248:**547–552.

18. **Brachmann, A., G. Weinzierl, J. Kämper, and R. Kahmann.** 2001. Identification of genes in the bW/bE regulatory cascade in *Ustilago maydis*. Mol. Microbiol. **42:**1047–1063.

19. **Brett, C. L., M. Donowitz, and R. Rao.** 2005. Evolutionary origins of eukaryotic sodium/proton exchangers. Am. J. Physiol. Cell Physiol. **288:**C223–C239.

20. **Brunelli, J. P., and M. L. Pall.** 1993. A series of yeast/*Escherichia coli* λ expression vectors designed for directional cloning of cDNAs and cre/lox-mediated plasmid excision. Yeast **9:**1309–1318.

21. **Carden, D. E., D. J. Walker, T. J. Flowers, and A. J. Miller.** 2003. Single-cell measurements of the contribution of cytosolic Na$^+$ and K$^+$ to salt tolerance. Plant Physiol. **131:**676–683.

22. **Föster, C., S. Marienfeld, R. Wilhelm, and R. Krämer.** 1998. Organelle purification and selective permeabilisation of the plasma membrane: two different approaches to study vacuoles of the filamentous fungus *Ashbya gossypii*. FEMS Microbiol. Lett. **167:**209–214.

23. **Gao, X. L., Z. H. Ren, Y. X. Zhao, and H. Zang.** 2003. Overexpression of *SOD2* increases salt tolerance of Arabidopsis. Plant Physiol. **133:**1873–1881.

24. **García, M. J., G. Ríos, R. Ali, J. M. Bellés, and R. Serrano.** 1997. Comparative physiology of salt tolerance in *Candida tropicalis* and *Saccharomyces cerevisiae*. Microbiology **143:**1125–1131.

25. **Garciadeblas, B., F. Rubio, F. J. Quintero, M. A. Bañuelos, and A. Rodríguez-Navarro.** 1993. Differential expression of two genes encoding isoforms of the ATPase involved in sodium efflux in *Saccharomyces cerevisiae*. Mol. Gen. Genet. **236:**363–368.

26. **Garciadeblás, B., M. E. Senn, M. A. Bañuelos, and A. Rodríguez-Navarro.** 2003. Sodium transport and HKT transporters: the rice model. Plant J. **34:**788–801.

27. **Gillissen, B., J. Bergemann, C. Sandmann, B. Schrör, M. Bölker, and R. Kahmann.** 1992. A two-component regulatory system for self/non-self recognition in *Ustilago maydis*. Cell **68:**647–657.

28. **Hahnenberger, K. M., Z. Jia, and P. G. Young.** 1996. Functional expression of the *Schizosaccharomyces pombe* Na$^+$/H$^+$ antiporter gene, *sod2*, in *Saccharomyces cerevisiae*. Proc. Natl. Acad. Sci. USA **93:**5031–5036.

29. **Hamilton, R., C. K. Watanabe, and H. A. de Boer.** 1987. Compilation and comparison of the sequence context around the AUG start codons in *Saccharomyces cerevisiae* mRNAs. Nucleic Acid Res. **15:**3581–3593.

30. **Holliday, R.** 1974. *Ustilago maydis*, p. 575–595. *In* R. C. King (ed.), Handbook of genetics. Plenum Press, New York, NY.

31. **Iizumi, K., Y. Mikami, M. Hashimoto, T. Nara, Y. Hara, and T. Aoki.** 2006. Molecular cloning and characterization of ouabain-insensitive Na$^+$-ATPase in the parasitic protist *Trypanosoma cruzi*. Biochim. Biophys. Acta **1758:**738–746.

32. **Jacobs, A., C. Lunde, A. Bacic, M. Tester, and U. Roessner.** 2007. The impact of constitutive heterologous expression of a moss Na$^+$ transporter on the metabolomes of rice and barley. Metabolomics **3:**307–317.

33. **Jorgensen, P. L., K. O. Hakansson, and S. J. D. Karlish.** 2003. Structure and mechanism of Na,K-ATPase: functional sires and their interactions. Annu. Rev. Physiol. **65:**817–849.

34. **Juárez, O., G. Guerra, F. Martínez, and J. P. Pardo.** 2004. The mitochondrial respiratory chain of *Ustilago maydis*. Biochim. Biophys. Acta **1658:**244–251.

35. **Kahmann, R., and J. Kämper.** 2004. *Ustilago maydis*: how its biology relates to pathogenic development. New Phytol. **164:**31–42.

36. **Kämper, J., R. Kahmann, M. Bölker, L.-J. Ma, T. Brefort, B. S. Saville, F. Banuett, J. W. Kronstad, S. E. Gold, O. Müller, M. H. Perlin, H. A. B. Wösten, R. de Vries, et al.** 2006. Insights from the genome of the biotrophic fungal plant pathogen *Ustilago maydis*. Nature **444:**97–101.

37. **Kogej, T., J. Ramos, A. Plemenitas, and N. Gunde-Cimerman.** 2005. The halophilic fungus *Hortaea werneckii* and the halotolerant fungus *Aureobasidium pullulans* maintain low intracellular cation concentrations in hypersaline environments. Appl. Environ. Microbiol. **71:**6600–6605.

38. **Martínez-Espinosa, A. D., J. Ruiz-Herrera, C. G. León-Ramírez, and S. E. Gold.** 2004. MAP kinases and cAMP signaling pathways modulate the pH-induced yeast-to-mycelium dimorphic transition in the corn smut fungus *Ustilago maydis*. Curr. Microbiol. **49:**274–281.

39. **Montiel, V., and J. Ramos.** 2007. Intracellular Na$^+$ and K$^+$ distribution in *Debaryomyces hansenii*. Cloning and expression in *Saccharomyces cerevisiae* of *DhNHX1*. FEMS Yeast Res. **7:**102–109.

40. **Müller, P., C. Aichinger, N. Feldbrugge, and R. Kahmann.** 1999. The MAP kinase *kpp2* regulates mating and pathogenic development in *Ustilago maydis*. Mol. Microbiol. **34:**1007–1017.

41. **Nakayama, H., K. Yoshida, and A. Shinmyo.** 2004. Yeast plasma membrane Ena1p ATPase alters alkali-cation homeostasis and confers increased salt tolerance in tobacco cultured cells. Biotechnol. Bioeng. **85:**776–789.

42. **Nishikawa, T., H. Aiba, and T. Mizuno.** 1999. The cta3$^+$ gene that encodes a cation-transporting P-type ATPase is induced by salt stress under control of the Wis1-StyI MAPKK-MAPK cascade in fission yeast. FEBS Lett. **455:**183–187.

43. **Padan, E., E. Bibi, M. Ito, and T. A. Krulwich.** 2005. Alkaline pH homeostasis in bacteria: new insights. Biochim. Biophys. Acta **1717:**67–88.

44. **Quintero, F. J., B. Garciadeblás, and A. Rodríguez-Navarro.** 1996. The *SAL1* gene of Arabidopsis, encoding an enzyme with 3′(2′),5′-bisphosphate nucleotidase and inositol polyphosphatase 1-phosphatase activities, increases salt tolerance in yeast. Plant Cell **8:**529–537.

45. **Radchenko, M. V., K. Tanaka, R. Waditee, S. Oshimi, Y. Matsuzaki, M. Fukuhara, H. Kobayashi, T. Takabe, and T. Nakamura.** 2006. Potassium/proton antiport system of *Escherichia coli*. J. Biol. Chem. **281:**19822–19829.

46. **Ramos, J., R. Haro, and A. Rodríguez-Navarro.** 1990. Regulation of potassium fluxes in *Saccharomyces cerevisiae*. Biochim. Biophys. Acta **1029:**211–217.

47. **Rodríguez-Navarro, A.** 2000. Potassium transport in fungi and plants. Biochim. Biophys. Acta **1469:**1–30.

48. **Rodríguez-Navarro, A., and J. Ramos.** 1984. Dual system for potassium transport in *Saccharomyces cerevisiae*. J. Bacteriol. **159:**940–945.

49. **Ruiz, A., and J. Ariño.** 2007. Function and regulation of the *Saccharomyces cerevisiae ENA* sodium ATPase system. Eukaryot. Cell **6:**2175–2183.

50. **Scarborough, G. A.** 2002. Molecular mechanism of the P-type ATPases. J. Bioenerg. Biomembr. **34:**235–250.

51. **Sherman, F.** 1991. Getting started with yeast. Methods Enzymol. **194:**3–21.

52. **Slayman, C. W., and E. L. Tatum.** 1964. Potassium transport in *Neurospora*. I. Intracellular sodium and potassium concentrations, and cation requirements for growth. Biochim. Biophys. Acta **88:**578–592.

53. **Tester, M., and R. Davenport.** 2003. Na$^+$ tolerance and Na$^+$ transport in higher plants. Ann. Bot. **91:**503–527.

54. **Thompson, J. D.** 1997. The CLUSTAL_X windows interface: flexible strategies for multiple sequence alignment aided by quality analysis tools. Nucleic Acids Res. **25:**4876–4882.

55. **Venema, K., A. Belver, M. C. Marín-Manzano, M. P. Rodríguez-Rosales, and J. P. Donaire.** 2003. A novel intracellular K$^+$/H$^+$ antiporter related to Na$^+$/H$^+$ antiporters is important for K$^+$ ion homeostasis in plants. J. Biol. Chem. **278:**22453–22459.

56. **Wedlich-Söldner, R., I. Schulz, A. Straube, and G. Steinberg.** 2002. Dynein supports motility of endoplasmic reticulum in the fungus *Ustilago maydis*. Mol. Biol. Cell **13:**965–977.

57. **Zhao, F., S. L. Guo, H. Zang, and Y. X. Zhao.** 2006. Expression of yeast SOD2 in transgenic rice results in increased salt tolerance. Plant Sci. **170:**216–224.